Helical donor-acceptor platinum complexes displaying dual luminescence and near-infrared circularly polarized luminescence

Pablo Vazquez-Dominguez, Oceane Journaud, Nicolas Vanthuyne, Denis Jacquemin, Ludovic Favereau, Jeanne Crassous, Abel Ros

Dalton Transactions

ROYAL SOCIETY OF CHEMISTRY

COMMUNICATION

View Article Online
View Journal | View Issue

Cite this: *Dalton Trans.*, 2021, **50**, 13220

Received 1st July 2021,
Accepted 10th September 2021

DOI: 10.1039/d1dt02184b

rsc.li/dalton

Helical donor–acceptor platinum complexes displaying dual luminescence and near-infrared circularly polarized luminescence†

Pablo Vázquez-Domínguez,[a] Océane Journaud,[b] Nicolas Vanthuyne,[c] Denis Jacquemin, *[d] Ludovic Favereau, *[b] Jeanne Crassous *[b] and Abel Ros *[a]

A series of chiral platina[5]helicenes displaying dual luminescence, *i.e.*, fluorescence between 450 and 600 nm and red/NIR phosphorescence between 700 and 900 nm, has been synthesised, characterised and studied by first-principle calculations. This unusual behavior has been attributed to limited electronic interactions between the d orbitals of the metal and the π-orbitals of the organic ligand on the excited-state. Accordingly, the electron richness of the donor group on the helical ligand does not affect the energy of the phosphorescence process but does play a role on its efficiency. Interestingly, near-infrared circularly polarized luminescence can be obtained for the three complexes with dissymmetry factors up to 3 × 10^{-3} at 750 nm.

The design of chiral π-conjugated materials that are able to interact specifically with a circularly polarized light (CP-Light) has recently attracted considerable attention due to the potential of the latter in the fields of (chir)optoelectronics including stereoscopic displays and organic light-emitting diodes (OLEDs), optical information processing, as well as in bioimaging and chiral sensing.[1] In this context, chiral lanthanide and chromium complexes have been intensively investigated for their high CP luminescence (CPL) intensity owing to their magnetically allowed transitions, resulting in luminescence dissymmetry factors, *i.e.*, $g_{lum} = 2(I_L - I_R)/(I_L + I_R)$, above unity,[2] and enable access to efficient near-infrared CPL emitters.[3] Recently, chiral organic and organometallic materials have received more attention as potential CP-Light absorbers and emitters due to their readily tuneable photo-physical and chiro-optical properties and their relatively simple integration in optoelectronic devices such as CP-OLEDs, chiral photovoltaics and transistors.[4] Although this class of compounds often displays higher luminescence quantum yields than lanthanide and chromium complexes thanks to their electronically allowed transitions, their CPL intensity dramatically decreases with typical g_{lum} falling in the 10^{-4} to 10^{-2} range.[5]

Accordingly, one of the major challenges for such CPL emitters is to identify the key electronic and structural factors controlling the CPL intensity, which would allow establishing molecular design rules leading to higher g_{lum} values.[6] Indeed, supramolecular assembly,[7] and other intermolecular approaches such as energy transfer, charge transfer and excimer involving chiral molecules have resulted in promising to impressive CPL values,[8] with g_{lum} up to 0.15,[9] opening new opportunities for chiral organic and organometallic materials.[5d] Despite this achievement, the development of far-red and near-infrared (NIR) molecular chiral emitters for bioimaging or optical data transmission remains a considerable challenge compared with the more classical blue, green and yellow CPL emitters.[10] Indeed, non-radiative deactivation pathways become more efficient as the gap becomes smaller, an effect commonly dubbed 'energy gap law' that is critical when reaching the NIR region. Several chiral compounds displaying chiro-optical properties beyond 600 nm have been reported, based for instance on extended helical π-systems;[11] however, only a few have shown a CPL over 700 nm (compounds **A** & **B**, Fig. 1).[12]

Moreover, the measured g_{lum} values in such emitters hardly exceed 1.0 × 10^{-3}, owing to the difficulty to efficiently combine a highly delocalized π-conjugated system with a chiral environment. In fact, the molecular CPL emitters displaying the most red-shifted response rely on a carbohelicene- or Schiff-platinum(II) complex, which afford g_{lum} of ±0.3 × 10^{-3} at 720 nm and ±2.8 × 10^{-3} at 731 nm, respectively (**C** & **D**, Fig. 1).[13] Indeed, using Pt complexes to generate NIR phosphorescence in chiral systems appears as a good strategy to generate NIR CPL activity.[13b,14] Furthermore, cyclometalated phosphorescent d^8 metal complexes containing π-conjugated ligands with

[a]*Institute for Chemical Research (CSIC-US), C/Américo Vespucio 49, E-41092 Seville, Spain. E-mail: abel.ros@iiq.csic.es*
[b]*Univ Rennes, CNRS, ISCR-UMR 6226, F-35000 Rennes, France. E-mail: ludovic.favereau@univ-rennes1.fr, jeanne.crassous@univ-rennes1.fr*
[c]*Aix Marseille University, CNRS, Centrale Marseille, iSm2, Marseille, France*
[d]*Laboratoire CEISAM, UMR 6230, CNRS, Université de Nantes, Nantes, France. E-mail: Denis.Jacquemin@univ-nantes.fr*

†Electronic supplementary information (ESI) available. See DOI: 10.1039/d1dt02184b

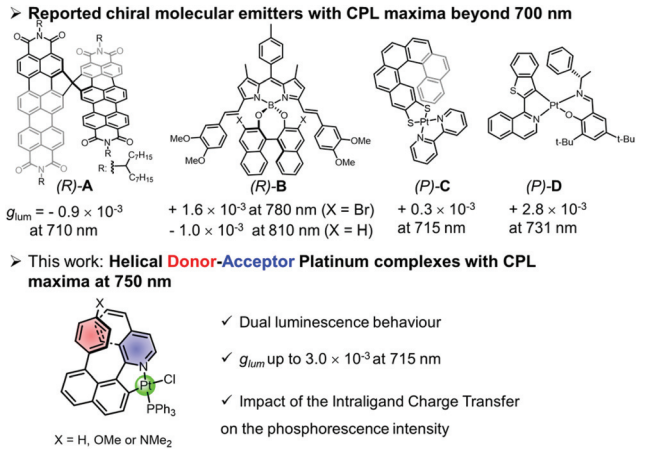

Fig. 1 Top: Chemical structures of the molecular CPL emitters displaying CPL maxima beyond 700 nm in solution (see ref. 8 and 9). Bottom: Chemical structures of the investigated helical donor–acceptor platinum(II) complexes in this report.

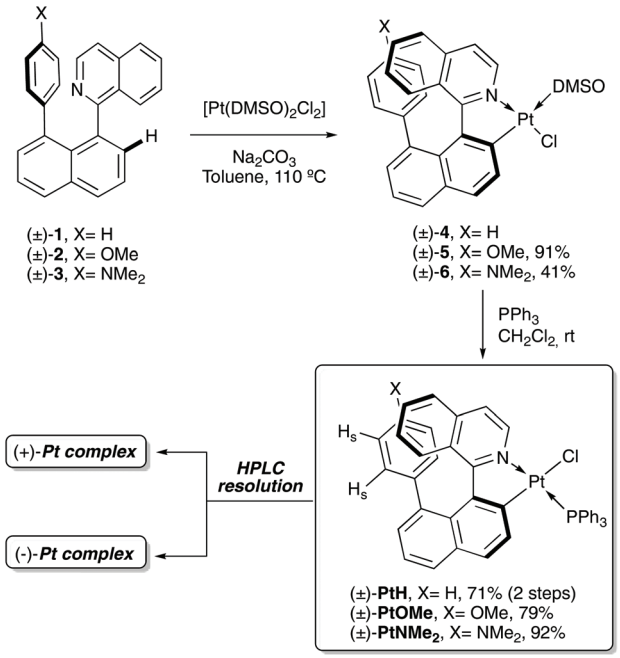

Scheme 1 Synthesis of [Pt(C,N)(PPh_3)Cl] complexes **PtH**, **PtOMe** and **$PtNMe_2$**.

N and/or C donor atoms have been extensively studied and used in the development of high-performance OLEDs.[13b,14c,15]

Following a previously developed method by some of us using cycloplatination to generate helical platinacycles displaying chirality from the helix and room temperature phosphorescence from the platinum,[16] herein, we explore a new approach towards the development of far-red and NIR chiral luminescent material based on a helical donor–acceptor π-conjugated structure incorporating a platinum metallic ion, namely, a push–pull platina[5]helicene. This new family of chiral organometallic complexes shows a dual emission process with a modulation of the chiro-optical and photo-physical properties resulting from the charge-transfer character of the helical organic ligand. Interestingly, increasing the electric dipole moment of the latter by tuning the donor substituent strength increases dramatically the efficiency of the phosphorescence process, which shows an emission maximum at 770 nm associated with a g_{lum} of 3.0×10^{-3}. Such intensity of NIR CPL is among the highest achieved so far at the molecular level and provides a platform for designing future chiral dyes showing responses in the low-energy region of the spectrum.

Synthesis and structural analysis (experimental and theoretical)

For the synthesis of the Pt-helicene complexes, a general cyclo-platination/ligand substitution two-step process was followed (Scheme 1). First, the cyclo-platination reaction of the axially chiral arylisoquinolines **1–3**[17] with [$Pt(DMSO)_2Cl_2$] under Na_2CO_3 (2 eq.)/toluene (reflux) conditions,[16c] gives the corresponding [Pt(C,N)(DMSO)Cl] complexes **4–5**, which can then be subjected to DMSO → PPh_3 ligand substitution to afford the desired platinahelicenes [$Pt(C,N)PPh_3Cl$][18] in 71%–92% yields after column chromatography on silica gel. The racemic mixtures were resolved using semi-preparative chiral HPLC separation to give the enantiopure complexes with ee's up to 99% (further details can be found in the ESI†).

Unfortunately, none of these complexes could be obtained as single crystal to be analysed by X-ray diffraction; however, the nuclear magnetic resonance (NMR) spectroscopy analysis in solution confirmed the formation of the expected complexes with a *trans*-N,P configuration. In more details, the ^{1}H NMR spectra show the deshielding of the isoquinoline *ortho*-C–H protons, which appear as a doublet of doublet at 9.50 ppm with a $^3J_{H,P} \sim 3.4$ Hz (see ESI†), and the ^{31}P NMR spectra exhibit a singlet peak around 22.7 ppm flanked by ^{195}Pt satellites signals with $^1J_{PtP} \sim 4300$ Hz, in accordance with similar [Pt(C,N)(PPh_3)Cl] complexes presenting a *trans* configuration between the phosphine moiety and the nitrogen atom.[19] Moreover, the spectra of the three complexes display a shielding of the aryl protons assigned to the substituent at the 8-position of the naphthalene fragment of the ligand (H_S, Scheme 1), owing to the π–π stacking with the isoquinoline moiety (see the ESI†). In the case of complex **PtH**, the formation of some amount of the *cis*-N,P isomer was observed (*ca.* 6 : 1 *trans*/*cis* mixture in $CDCl_3$). Curiously, when this NMR sample in $CDCl_3$ was heated at 40 °C, a slow evolution to the *cis*-N,P isomer was observed. The same isomerization was instantly achieved by dissolving the *trans*-complex in acetone, as evidenced by the corresponding ^{1}H NMR spectra (see the ESI†).[20] The reverse *cis*-to-*trans* N,P isomerization could also be observed by dissolving the *cis*-N,P isomer in CD_2Cl_2 and heating at 40 °C for two days.[21]

Photo-physical and chiro-optical properties (experimental and theoretical)

Fig. 2 shows the ultraviolet–visible (UV–vis) absorption spectra of the helical platinum complexes, which display a similar pattern with two dominant bands between 300 and

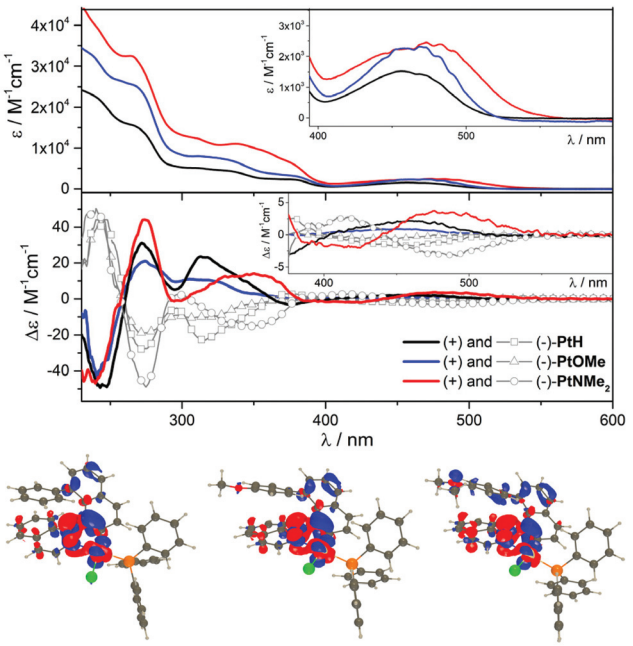

Fig. 2 Top: UV-Vis and ECD spectra for the (+) and (–) enantiomers of **PtH**, **PtOMe** and **PtNMe$_2$** in dichloromethane solutions. Bottom: EDD plots (contour 0.002 au) for the lowest dipole-allowed transition of **PtH**, **PtOMe** and **PtNMe$_2$** with the crimson (blueberry) lobes representing increase (decrease) of electron density upon photo-excitation (the difference between the total excited state and ground state densities, as computed with TD-DFT and DFT, respectively).

400 nm ($\varepsilon \sim 5$–10×10^3 M^{-1} cm^{-1}) and below 300 nm ($\varepsilon \sim 15$–30×10^3 M^{-1} cm^{-1}) that are assigned to $\pi \rightarrow \pi^*$ transitions and to an additional mixture of metal-to-ligand (ML) and intra-ligand (IL) charge-transfer excitations for the low-energy one (for comparison, the UV-vis spectra of the corresponding organic ligands are depicted in Fig. S4†). The weaker band between 400 and 550 nm ($\varepsilon \sim 1.5$–2.5×10^3 M^{-1} cm^{-1}), corresponding to the lowest energy excitation, involves charge-transfer (CT) transitions arising mainly from the metal to the isoquinoline ligand, with also a contribution of the naphthyl-substituted unit (ILCT transitions, Fig. 2). In the case of the latter, replacing a phenyl ring with a stronger *N*,*N*-dimethylaniline donor group greatly increases the intensity of the absorption throughout the whole spectrum and induces a small redshift of *ca.* 20 nm of the lowest energy band, which confirms the occurrence of ILCT for this excitation in addition to the classical MLCT. According to Time-Dependent Density Functional Theory (TD-DFT) calculations, the lowest vertical excitation of **PtH**, **PtOMe**, and **PtNMe$_2$** appear at 403, 408, and 421 nm, respectively. These values are blue-shifted as compared with the experimental results, which is the logical consequence of neglecting the vibronic couplings in the calculation. More importantly, the trend in the series with the *ca.* 20 nm redshift between **PtH** and **PtOMe** is reproduced. The electron density difference (EDD) plots for these lowest transitions are displayed in Fig. 2. As can be seen, the transitions involve both the ligand and the metal, the amino group playing a non-negligible donating role in **PtNMe$_2$**.

Electronic circular dichroism (ECD) of the investigated complexes further highlights the differences related to the nature of the substituent at the 8-position of the naphthalene fragment.

Although the three complexes show similar ECD signals in the high energy region, with a positive → negative couplet at 260 nm for the (+)-enantiomers (Fig. 2) attributed to the binaphthyl ECD-type signature,[22] the low energy part of the spectra (between 300 and 550 nm), appears more redshifted for (+)-**PtNMe$_2$** than for (+)-**PtOMe** and (+)-**PtH**. In fact, the set of three signals at 320, 375 and 450 nm for the two latter compounds, respectively positive, negative and positive, are found at 350, 415, and 484 nm in the case of (+)-**PtNMe$_2$**, which evidences the impact of the donor strength in these optical transitions.

Overall, this combined experimental and theoretical study shows that the metal significantly interacts with the helical π-conjugated system in the ground-state, explaining their optical properties. Expectedly, the role of the platinum atom is not only to stabilise the helical configuration but also to modify the electronic and chiro-optical properties of the organic donor–acceptor system.[16] Such aspect is also clearly observed in the emissive properties of these new chiral derivatives. Indeed, the three complexes display a dual emission process with a fluorescence emission between 450 and 600 nm and red/NIR phosphorescence between 700 and 900 nm in diluted degassed solutions. Further experimental evidences of both fluorescence and phosphorescence emissions have been obtained by recording the luminescence response of the complexes under air atmosphere, which shows only a decrease of the NIR signal due to the quenching of the emitting triplet state by molecular oxygen. In addition, lifetime measurements indicate a decay of few nanoseconds for the high energy emission and of several hundred nanoseconds for the lower energy emission (Table 1 and ESI†). All these aspects confirm the assignments of the fluorescence and phosphorescence emissions.

Such behaviour has been previously observed for platinum complexes exhibiting a weak electronic interaction between the d orbitals of the metal and the π-orbitals of the organic ligand.[23] The observation of this dual luminescence suggests that this feature is present in the excited state of the present complexes. The theoretical calculations are consistent with these observations since vertical emission wavelengths at 523, 523, and 543 nm were obtained for **PtH**, **PtOMe**, and **PtNMe$_2$**, respectively, by TD-DFT while U-DFT calculations predict vertical phosphorescence at 872, 862, and 871 nm for the same three derivatives. According to the calculations, these triplets are mainly ligand-centred with trifling role of the substituent (H, OMe, NMe$_2$, see Fig. 3), which explains why the phosphorescence energies of the three dyes are more similar than their fluorescence counterparts. Interestingly, the intensity of the NIR phosphorescence increases significantly when going from the phenyl to the *N*,*N*-dimethylaniline donor substituent,

Table 1 Photo-physical and chiro-optical data for the **PtH**, **PtOMe** and **PtNMe$_2$** complexes

	Complex (+)-**PtH**	Complex (+)-**PtOMe**	Complex (+)-**PtNMe$_2$**
λ_{abs} [a]/nm (ε/ M^{-1} cm^{-1})	458 (1530), 373 (2265), 310 (5273), 266 (15 615)	465 (2294), 373 (3800), 310 (8055), 266 (25 501)	475 (2430), 373 (6968), 336 (10 963), 310 (12 430), 264 (32 682)
λ_{ECD} [a]/nm ($\Delta\varepsilon$/ M^{-1} cm^{-1})	454 (+2), 377 (−4), 312 (+23), 271 (+31), 243 (−48)	448 (+1), 381 (−0.5), 305 (+11), 274 (+21), 241 (−41)	484 (+4), 415 (−2), 350 (+14), 296 (−1), 274 (+44), 238 (−46)
λ_{em} [b] (nm)/ ΔE_{ST} [c]	520_{Fl}, 765_{Ph}/0.75	565_{Fl}, 770_{Ph}/0.73	590_{Fl}, 780_{Ph}/0.65
ϕ_{Lum} [b] (%)	<1	<1	<1
τ_{Lum} [b] [ns]	4.0 ns (28%) & 18.5 ns (72%) (560 nm, fluo.); 22.0 ns (26%) & 248.9 ns (74%) (770 nm, phos.)	3.2 ns (45%) & 23.4 ns (55%) (560 nm, fluo.); 19.4 ns (4%) & 382.7 ns (96%) (770 nm, phos.)	4.2 ns (580 nm, fluo.); 411 ns (770 nm, phos.)
$\lvert g_{lum}\rvert$ [b] ($\times 10^3$)	2.5×10^{-3}	3.0×10^{-3}	3.0×10^{-3}

[a] In dichloromethane at 298 K. [b] In toluene at 298 K. [c] The experimental S_1–T_1 gaps of the complexes have been estimated from the luminescence spectra with the values of S_1 and T_1 obtained from the onsets of the fluorescence and phosphorescence bands, respectively (Fig. 4).

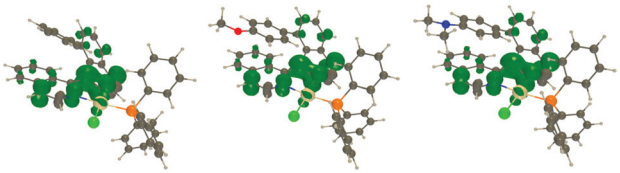

Fig. 3 Spin density difference plots (contour 0.005 au) of the lowest triplet state of **PtH**, **PtOMe** and **PtNMe$_2$** at its optimal geometry.

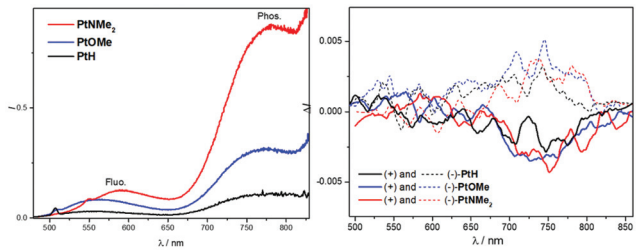

Fig. 4 (a) Luminescence and CPL spectra of the PtH (black line), PtOMe (blue line) and PtNMe$_2$ (red line) complexes measured in toluene solution. Note that the raise of the signal at 820 nm is due to the limited sensitivity of the fluorimeter photodetector.

suggesting an important role of the CT character of the ligand in the efficiency of this emission. Low photoluminescence quantum yields have been measured for the three complexes (>1%, Table 1), owing to probably high non-radiative rates arising from the presence of the monodentate ligands, along with the classically 'energy gap law' effect.

To gain further insights on this luminescence behaviour, theoretical calculations were performed. It is generally admitted that inter-system crossing (ISC) takes place after relaxation to the lowest S_1 state. At the optimal S_1 geometry, there is only one triplet lower in energy than S_1 according to theory. The experimental S_1–T_1 gaps have been experimentally estimated to 0.75, 0.73 and 0.65 eV for **PtH**, **PtOMe** and **PtNMe$_2$**, respectively, following the trend obtained for the computed ones, *i.e.*, 0.92, 0.92, and 0.59 eV for **PtH**, **PtOMe** and **PtNMe$_2$**, respectively, indicating that ISC should be facilitated for **PtNMe$_2$** as the S–T gap is clearly the smallest. The computed spin–orbit coupling matrix elements (SOCMEs) for the S_1–T_1 transition are 17, 14 and 7 cm^{-1} in **PtH**, **PtOMe** and **PtNMe$_2$**, respectively. While remaining moderate for a Pt-complex, which is consistent with the limited involvement of the metal in the excitation, these values are clearly large enough to induce ISC. This can be viewed as an intermediate situation, in which the rather large gaps make the ISC sufficiently slow to allow for radiative decay from S_1 (fluorescence), while the non-trifling but not large SOCMEs allow for ISC. This is consistent with the experimental findings of dual emission. At the optimal T_1 geometry, from which phosphorescence occurs, the SOCMEs for the T_1–S_0 process are very similar for the three dyes: 27, 24 and 24 cm^{-1} for **PtH**, **PtOMe** and **PtNMe$_2$**, respectively, consistent with the density plots displayed in Fig. 3; therefore, the different behaviours noted experimentally should originate from various ISC kinetics rather than from different efficiencies in the actual phosphorescence radiative process.

The circularly polarized luminescence for each enantiomer of **PtH**, **PtOMe** and **PtNMe$_2$** was recorded in degassed toluene solutions, affording mirror-image signals corresponding only to the NIR phosphorescence emission, which can be probably explained by the weak efficiency of the fluorescence process (Fig. 4).

On the basis of the obtained reliable signals, similar g_{lum} factors of *ca.* 2.5–3 × 10^{-3} for the three complexes were obtained. The three complexes exhibit a negative CPL response for the (+)-enantiomer, and their lowest ECD signals are positive, which indicates that different transitions are involved in the absorption and emission phenomena. Although the recorded g_{lum} values are similar to those of classical molecular CPL emitters,[1c,5a,c] the obtained NIR spectra are among the most red-shifted reported to date for chiral luminophores based on organic and platinum complexes. Especially, the combination of a strong push–pull organic ligand with metallic complexes appears an interesting approach for reaching far red and NIR emission.

Conclusions

In conclusion, we described here the synthesis of a new family of helical platinum(II) complexes bearing donating or accepting substituents within the helical organic ligand, and the joint experimental and theoretical investigation of their chiro-optical and photo-physical properties. We showed that the combination of platinum ion with an organic ligand possessing intramolecular charge-transfer abilities results in a dual luminescence behaviour with phosphorescence emission in the NIR region. Interestingly, the strength of the donor group on the helical ligand does not affect the energy of this emission process but rather plays a role on its efficiency through the tuning of the S–T gap and therefore of the ISC process. The three complexes exhibit corresponding CP phosphorescence with g_{lum} of 3×10^{-3}, which is a significant value for this low energy region. We hope that this investigation may offer new opportunities to design innovative and efficient NIR CPL emitters.

Conflicts of interest

There are no conflicts to declare.

Acknowledgements

L. F. and J. C. acknowledge the Ministère de l'Education Nationale, de la Recherche et de la Technologie and the Centre National de la Recherche Scientifique (CNRS). A. R. acknowledges the Spanish Ministerio de Ciencia e Innovación (Grants PID2019-106358GB-C21 and PID2019-106358GB-C22), European funding (ERDF), Junta de Andalucía (FQM-263 group). The PRISM core facility (Biogenouest©, UMS Biosit, Université de Rennes 1 – Campus de Villejean – 35043 RENNES Cedex, FRANCE) is acknowledged for the NMR characterizations and ECD measurements. The Caphter facility (ScanMAT, UMS 2001, Université de Rennes 1 – Campus de Beaulieu) is acknowledged for the photoluminescence characterizations of the compounds. This work used the computational resources of the CCIPL center installed in Nantes.

Notes and references

1 (*a*) M. Lindemann, G. Xu, T. Pusch, R. Michalzik, M. R. Hofmann, I. Žutić and N. C. Gerhardt, *Nature*, 2019, **568**, 212–215; (*b*) H. Wang, L. Liu and C. Lu, *Procedia Comput. Sci.*, 2018, **131**, 511–519; (*c*) J. M. Han, S. Guo, H. Lu, S. J. Liu, Q. Zhao and W. Huang, *Adv. Opt. Mater.*, 2018, **6**, 1800538; (*d*) T. Novikova, A. Pierangelo, S. Manhas, A. Benali, P. Validire, B. Gayet and A. D. Martino, *Appl. Phys. Lett.*, 2013, **102**, 241103; (*e*) B. Kunnen, C. Macdonald, A. Doronin, S. Jacques, M. Eccles and I. Meglinski, *J. Biophotonics*, 2015, **8**, 317–323; (*f*) R. Carr, N. H. Evans and D. Parker, *Chem. Soc. Rev.*, 2012, **41**, 7673–7686; (*g*) L. E. MacKenzie and R. Pal, *Nat. Rev. Chem.*, 2020, **5**, 109–124.

2 (*a*) F. Zinna and L. Di Bari, *Chirality*, 2015, **27**, 1–13; (*b*) E. R. Neil and D. Parker, *RSC Adv.*, 2017, **7**, 4531–4540; (*c*) S. Shuvaev, M. A. Fox and D. Parker, *Angew. Chem., Int. Ed.*, 2018, **57**, 7488–7492; (*d*) F. Zinna, M. Pasini, F. Galeotti, C. Botta, L. Di Bari and U. Giovanella, *Adv. Funct. Mater.*, 2017, **27**, 1603719; (*e*) J. R. Jiménez, B. Doistau, C. M. Cruz, C. Besnard, J. M. Cuerva, A. G. Campaña and C. Piguet, *J. Am. Chem. Soc.*, 2019, **141**, 13244–13252; (*f*) J. R. Jiménez, M. Poncet, S. Miguez-Lago, S. Grass, J. Lacour, C. Besnard, J. M. Cuerva, A. G. Campaña and C. Piguet, *Angew. Chem.*, 2021, **60**, 10095–10102.

3 (*a*) C. Dee, F. Zinna, W. R. Kitzmann, G. Pescitelli, K. Heinze, L. Di Bari and M. Seitz, *Chem. Commun.*, 2019, **55**, 13078–13081; (*b*) R. S. Dickins, J. A. K. Howard, C. L. Maupin, J. M. Moloney, D. Parker, J. P. Riehl, G. Siligardi and J. A. G. Williams, *Chem. – Eur. J.*, 1999, **5**, 1095–1105; (*c*) C. L. Maupin, R. S. Dickins, L. G. Govenlock, C. E. Mathieu, D. Parker, J. A. G. Williams and J. P. Riehl, *J. Phys. Chem. A*, 2000, **104**, 6709–6717; (*d*) F. Zinna, L. Arrico and L. Di Bari, *Chem. Commun.*, 2019, **55**, 6607–6609; (*e*) B. Lefeuvre, C. A. Mattei, J. F. Gonzalez, F. Gendron, V. Dorcet, F. Riobé, C. Lalli, B. Le Guennic, O. Cador, O. Maury, S. Guy, A. Bensalah-Ledoux, B. Baguenard and F. Pointillart, *Chem. – Eur. J.*, 2021, **27**, 7362–7366.

4 (*a*) J. Gilot, R. Abbel, G. Lakhwani, E. W. Meijer, A. P. H. J. Schenning and S. C. J. Meskers, *Adv. Mater.*, 2010, **22**, E131–E134; (*b*) Y. Yang, R. C. da Costa, M. J. Fuchter and A. J. Campbell, *Nat. Photonics*, 2013, **7**, 634–638; (*c*) Y. Yang, R. C. da Costa, D.-M. Smilgies, A. J. Campbell and M. J. Fuchter, *Adv. Mater.*, 2013, **25**, 2624–2628; (*d*) J. R. Brandt, X. Wang, Y. Yang, A. J. Campbell and M. J. Fuchter, *J. Am. Chem. Soc.*, 2016, **138**, 9743–9746; (*e*) S. Feuillastre, M. Pauton, L. Gao, A. Desmarchelier, A. J. Riives, D. Prim, D. Tondelier, B. Geffroy, G. Muller, G. Clavier and G. Pieters, *J. Am. Chem. Soc.*, 2016, **138**, 3990–3993; (*f*) M. Schulz, M. Mack, O. Kolloge, A. Lutzen and M. Schiek, *Phys. Chem. Chem. Phys.*, 2017, **19**, 6996–7008; (*g*) P. Josse, L. Favereau, C. Shen, S. Dabos-Seignon, P. Blanchard, C. Cabanetos and J. Crassous, *Chem. – Eur. J.*, 2017, **23**, 6277–6281; (*h*) J. R. Brandt, F. Salerno and M. J. Fuchter, *Nat. Rev. Chem.*, 2017, **1**, 0045; (*i*) L. Frederic, A. Desmarchelier, L. Favereau and G. Pieters, *Adv. Funct. Mater.*, 2021, **31**, 2010281; (*j*) K. Dhbaibi, L. Favereau, M. Srebro-Hooper, C. Quinton, N. Vanthuyne, L. Arrico, T. Roisnel, B. Jamoussi, C. Poriel, C. Cabanetos, J. Autschbach and J. Crassous, *Chem. Sci.*, 2020, **11**, 567–576; (*k*) K. Dhbaibi, L. Abella, S. Meunier-Della-Gatta, T. Roisnel, N. Vanthuyne, B. Jamoussi, G. Pieters, B. Racine, E. Quesnel, J. Autschbach, J. Crassous and L. Favereau, *Chem. Sci.*, 2021, **12**, 5522–5533; (*l*) D. W. Zhang, M. Li and C. F. Chen, *Chem. Soc. Rev.*, 2020, **49**, 1331–1343; (*m*) L. Zhou, G. Xie,

F. Ni and C. Yang, *Appl. Phys. Lett.*, 2020, **117**, 130502; (*n*) B. Doistau, J. R. Jimenez and C. Piguet, *Front. Chem.*, 2020, **8**, 555.

5 (*a*) H. Tanaka, Y. Inoue and T. Mori, *ChemPhotoChem*, 2018, **2**, 386–402; (*b*) W.-L. Zhao, M. Li, H.-Y. Lu and C.-F. Chen, *Chem. Commun.*, 2019, **55**, 13793–13803; (*c*) L. Arrico, L. Di Bari and F. Zinna, *Chem. – Eur. J.*, 2021, **27**, 2920–2934; (*d*) J. Greenfield, J. Wade, J. Brandt, X. Shi, T. Penfold and M. Fuchter, *Chem. Sci.*, 2021, **12**, 8589–8602.

6 (*a*) G. Longhi, E. Castiglioni, J. Koshoubu, G. Mazzeo and S. Abbate, *Chirality*, 2016, **28**, 696–707; (*b*) H. Tanaka, M. Ikenosako, Y. Kato, M. Fujiki, Y. Inoue and T. Mori, *Commun. Chem.*, 2018, **1**, 38; (*c*) C. Schaack, L. Arrico, E. Sidler, M. Gorecki, L. Di Bari and F. Diederich, *Chem. – Eur. J.*, 2019, **25**, 8003–8007; (*d*) Y. Liu, Q. Xu, J. Sun, L. Wang, D. He, M. Wang and C. Yang, *Spectrochim. Acta, Part A*, 2020, **239**, 118475; (*e*) K. Tani, R. Imafuku, K. Miyanaga, M. E. Masaki, H. Kato, K. Hori, K. Kubono, M. Taneda, T. Harada, K. Goto, F. Tani and T. Mori, *J. Phys. Chem. A*, 2020, **124**, 2057–2063.

7 (*a*) J. N. Wilson, W. Steffen, T. G. McKenzie, G. Lieser, M. Oda, D. Neher and U. H. F. Bunz, *J. Am. Chem. Soc.*, 2002, **124**, 6830–6831; (*b*) Y. Geng, A. Trajkovska, S. W. Culligan, J. J. Ou, H. M. P. Chen, D. Katsis and S. H. Chen, *J. Am. Chem. Soc.*, 2003, **125**, 14032–14038; (*c*) H. Tsumatori, T. Nakashima and T. Kawai, *Org. Lett.*, 2010, **12**, 2362–2365; (*d*) D. Di Nuzzo, C. Kulkarni, B. Zhao, E. Smolinsky, F. Tassinari, S. C. J. Meskers, R. Naaman, E. W. Meijer and R. H. Friend, *ACS Nano*, 2017, **11**, 12713–12722; (*e*) M. Gon, R. Sawada, Y. Morisaki and Y. Chujo, *Macromolecules*, 2017, **50**, 1790–1802; (*f*) C. Kulkarni, D. Di Nuzzo, E. W. Meijer and S. C. J. Meskers, *J. Phys. Chem. B*, 2017, **121**, 11520–11527.

8 (*a*) T. Zhao, J. Han, P. Duan and M. Liu, *Acc. Chem. Res.*, 2020, **53**, 1279–1292; (*b*) L. Ji, Y. Sang, G. Ouyang, D. Yang, P. Duan, Y. Jiang and M. Liu, *Angew. Chem., Int. Ed.*, 2019, **58**, 844–848; (*c*) J. Han, D. Yang, X. Jin, Y. Jiang, M. Liu and P. Duan, *Angew. Chem., Int. Ed.*, 2019, **58**, 7013–7019; (*d*) D. Yang, P. Duan and M. Liu, *Angew. Chem., Int. Ed.*, 2018, **57**, 9357–9361; (*e*) J. Han, P. Duan, X. Li and M. Liu, *J. Am. Chem. Soc.*, 2017, **139**, 9783–9786; (*f*) A. Homberg, E. Brun, F. Zinna, S. Pascal, M. Górecki, L. Monnier, C. Besnard, G. Pescitelli, L. Di Bari and J. Lacour, *Chem. Sci.*, 2018, **9**, 7043–7052; (*g*) F. Zinna, E. Brun, A. Homberg and J. Lacour, in *Circularly Polarized Luminescence of Isolated Small Organic Molecules*, ed. T. Mori, Springer Singapore, Singapore, 2020, pp. 273–292, DOI: 10.1007/978-981-15-2309-0_12.

9 J. Wade, J. R. Brandt, D. Reger, F. Zinna, K. Y. Amsharov, N. Jux, D. L. Andrews and M. J. Fuchter, *Angew. Chem.*, 2021, **60**, 222–227.

10 X. Li, Y. Xie and Z. Li, *Adv. Photonics Res.*, 2021, **2**, 2000136.

11 (*a*) K. Dhbaibi, L. Favereau, M. Srebro-Hooper, M. Jean, N. Vanthuyne, F. Zinna, B. Jamoussi, L. Di Bari, J. Autschbach and J. Crassous, *Chem. Sci.*, 2018, **9**, 735–742; (*b*) K. Dhbaibi, C. Shen, M. Jean, N. Vanthuyne, T. Roisnel, M. Górecki, B. Jamoussi, L. Favereau and J. Crassous, *Front. Chem.*, 2020, **8**, 237–237; (*c*) R. Duwald, J. Bosson, S. Pascal, S. Grass, F. Zinna, C. Besnard, L. Di Bari, D. Jacquemin and J. Lacour, *Chem. Sci.*, 2020, **11**, 1165–1169; (*d*) J. Bosson, G. M. Labrador, C. Besnard, D. Jacquemin and J. Lacour, *Angew. Chem.*, 2021, **60**, 8733–8738; (*e*) R. Tarrieu, I. Hernandez Delgado, F. Zinna, V. Dorcet, S. Colombel-Rouen, C. Crévisy, O. Basle, J. Bosson and J. Lacour, *Chem. Commun.*, 2021, **57**, 3793–3796; (*f*) J. Bosson, G. M. Labrador, S. Pascal, F. A. Miannay, O. Yushchenko, H. Li, L. Bouffier, N. Sojic, R. C. Tovar, G. Muller, D. Jacquemin, A. D. Laurent, B. Le Guennic, E. Vauthey and J. Lacour, *Chem. – Eur. J.*, 2016, **22**, 18394–18403; (*g*) I. H. Delgado, S. Pascal, A. Wallabregue, R. Duwald, C. Besnard, L. Guenee, C. Nancoz, E. Vauthey, R. C. Tovar, J. L. Lunkley, G. Muller and J. Lacour, *Chem. Sci.*, 2016, **7**, 4685–4693; (*h*) R. Duwald, S. Pascal, J. Bosson, S. Grass, C. Besnard, T. Bürgi and J. Lacour, *Chem. – Eur. J.*, 2017, **23**, 13596–13601.

12 (*a*) J. Feng, L. Fu, H. Geng, W. Jiang and Z. Wang, *Chem. Commun.*, 2020, **56**, 912–915; (*b*) J. Jiménez, C. Díaz-Norambuena, S. Serrano, S. C. Ma, F. Moreno, B. L. Maroto, J. Bañuelos, G. Muller and S. de la Moya, *Chem. Commun.*, 2021, **57**, 5750–5753.

13 (*a*) T. Biet, T. Cauchy, Q. Sun, J. Ding, A. Hauser, P. Oulevey, T. Bürgi, D. Jacquemin, N. Vanthuyne, J. Crassous and N. Avarvari, *Chem. Commun.*, 2017, **53**, 9210–9213; (*b*) G. Fu, Y. He, W. Li, B. Wang, X. Lü, H. He and W.-Y. Wong, *J. Mater. Chem. C*, 2019, **7**, 13743–13747.

14 (*a*) Y. Zhang, Y. Wang, J. Song, J. Qu, B. Li, W. Zhu and W.-Y. Wong, *Adv. Opt. Mater.*, 2018, **6**, 1800466; (*b*) A. Zampetti, A. Minotto and F. Cacialli, *Adv. Funct. Mater.*, 2019, **29**, 1807623; (*c*) K. Zhang, T. Y. Wang, T. W. Wu, Z. M. Ding, Q. Zhang, W. G. Zhu and Y. Liu, *J. Mater. Chem. C*, 2021, **9**, 2282–2290.

15 K. Tuong Ly, R.-W. Chen-Cheng, H.-W. Lin, Y.-J. Shiau, S.-H. Liu, P.-T. Chou, C.-S. Tsao, Y.-C. Huang and Y. Chi, *Nat. Photonics*, 2017, **11**, 63–69.

16 (*a*) L. Norel, M. Rudolph, N. Vanthuyne, J. A. G. Williams, C. Lescop, C. Roussel, J. Autschbach, J. Crassous and R. Réau, *Angew. Chem., Int. Ed.*, 2010, **49**, 99–102; (*b*) N. Saleh, C. Shen and J. Crassous, *Chem. Sci.*, 2014, **5**, 3680–3694; (*c*) C. Shen, E. Anger, M. Srebro, N. Vanthuyne, K. K. Deol, T. D. Jefferson, G. Muller, J. A. G. Williams, L. Toupet, C. Roussel, J. Autschbach, R. Reau and J. Crassous, *Chem. Sci.*, 2014, **5**, 1915–1927; (*d*) E. Anger, M. Rudolph, L. Norel, S. Zrig, C. Shen, N. Vanthuyne, L. Toupet, J. A. G. Williams, C. Roussel, J. Autschbach, J. Crassous and R. Réau, *Chem. – Eur. J.*, 2011, **17**, 14178–14198.

17 Z. Domínguez, R. López-Rodríguez, E. Álvarez, S. Abbate, G. Longhi, U. Pischel and A. Ros, *Chem. – Eur. J.*, 2018, **24**, 12660–12668.

18 (*a*) V. V. Sivchik, A. I. Solomatina, Y.-T. Chen, A. J. Karttunen, S. P. Tunik, P.-T. Chou and I. O. Koshevoy, *Angew. Chem., Int. Ed.*, 2015, **54**, 14057–14060.

19 $^{1}J_{PtP} \sim 4300$ Hz values for phosphine ligand being trans to the N ligating atom, and $^{1}J_{PtP} \sim 2050$ Hz for the phosphine ligand trans to C. Some examples: (*a*) H. Samouei, M. Rashidi and F. W. Heinemann, *J. Iran. Chem. Soc.*, 2014, **11**, 1207–1216; (*b*) M. S. Sangari, M. G. Haghighi, S. M. Nabavizadeh, A. Pfitzner and M. Rashidi, *New J. Chem.*, 2018, **42**, 8661–8671.

20 (*a*) Y.-J. Kim, J.-I. Park, S.-C. Lee, K. Osakada, M. Tanabe, J.-C. Choi, T.-a. Koizumi and T. Yamamoto, *Organometallics*, 1999, **18**, 1349–1352; (*b*) A. Polo, J. Duran, R. Juanola, J. Real, J. Benet-Buchholz, M. Solà and A. Poater, *New J. Chem.*, 2017, **41**, 3015–3028.

21 (*a*) D. Mendola, N. Saleh, N. Vanthuyne, C. Roussel, L. Toupet, F. Castiglione, T. Caronna, A. Mele and J. Crassous, *Angew. Chem., Int. Ed.*, 2014, **53**, 5786–5790; (*b*) D. Mendola, N. Saleh, N. Hellou, N. Vanthuyne, C. Roussel, L. Toupet, F. Castiglione, F. Melone, T. Caronna, F. Fontana, J. Martí-Rujas, E. Parisini, L. Malpezzi, A. Mele and J. Crassous, *Inorg. Chem.*, 2016, **55**, 2009–2017.

22 (*a*) L. Di Bari, G. Pescitelli and P. Salvadori, *J. Am. Chem. Soc.*, 1999, **121**, 7998–8004; (*b*) N. Berova, L. D. Bari and G. Pescitelli, *Chem. Soc. Rev.*, 2007, **36**, 914–931.

23 (*a*) Y. Liu, H. Guo and J. Zhao, *Chem. Commun.*, 2011, **47**, 11471–11473; (*b*) Y. Y. Chia and M. G. Tay, *Dalton Trans.*, 2014, **43**, 13159–13168; (*c*) F. Geist, A. Jackel and R. F. Winter, *Dalton Trans.*, 2015, **44**, 3974–3987; (*d*) F. Geist, A. Jackel and R. F. Winter, *Inorg. Chem.*, 2015, **54**, 10946–10957.

